A general holographic insulator/superconductor model with dark matter sector away from the probe limit

Yan Peng^{1,2*}

¹ School of Mathematical Sciences, Qufu Normal University, Qufu, Shandong 273165, China and ² School of Mathematics and Computer Science, Shaanxi Sci-Tech University, Hanzhong, Shaanxi 723000, China

Qiyuan Pan^{3†}

³ Department of Physics, Key Laboratory of Low Dimensional Quantum Structures and Quantum Control of Ministry of Education, Hunan Normal University, Changsha, Hunan 410081, China

Yunqi Liu^{4‡}

⁴ School of Physics, Huazhong University of Science and Technology, Wuhan, Hubei 430074, China

Abstract

We investigate holographic phase transitions with dark matter sector in the AdS soliton background away from the probe limit. In cases of weak backreaction, we find that the larger coupling parameter α makes the gap of condensation shallower and the critical chemical potential keeps as a constant. In contrast, for very heavy backreaction, the dark matter sector could affect the critical chemical potential and the order of phase transitions. We also find the jump of the holographic topological entanglement entropy corresponds to a first order transition between superconducting states in this model with dark matter sector. More importantly, for certain sets of parameters, we observe novel phenomenon of retrograde condensation. In a word, the dark matter sector provides richer physics in the phase structure and the holographic superconductor properties are helpful in understanding dark matter.

PACS numbers: 11.25.Tq, 04.70.Bw, 74.20.-z

^{*} yanpengphy@163.com

panqiyuan@126.com

[‡] liuyunqi@hust.edu.cn

I. INTRODUCTION

The anti-de Sitter/conformal field theories (AdS/CFT) correspondence relates the strongly correlated conformal field theory on the boundary with a weakly interacting gravity system in the bulk [1–3]. According to this novel idea, the gauge/gravity duality has been successfully employed to gain a better understanding of the low energy physics in condensed matter systems from a higher dimensional gravitational dual. The simplest holographic metal/superconductor model dual to gravity theories was constructed by applying a scalar field and a Maxwell field coupled in the AdS black hole background [4–6]. And then the holographic insulator/superconductor transiton was also established in the AdS soliton spacetime [7, 8]. At present, a lot of more complete holographic superconductor models have been widely studied to model conductivity and other condensed matter physics properties in various gravity theories, such as the Einstein-Gauss-Bonnet gravity, Horava-Lifshitz gravity, non-linear electrodynamics gravity and so on, see Refs. [9]-[34].

According to contemporary astronomical observations, almost 24 percent of the total energy density in our universe is in the form of dark matter, whose configuration is still unclear. In order to model the dark matter, a new gravity was established by introducing an additional U(1) gauge field coupled to the normal Maxwell field [35, 36]. This dark matter gravity is strongly supported by astrophysical observation of 511 keV gamma rays [37] and the electron positron excess in galaxy [38, 39]. Moreover, this gravity reveals new physics allowing the 3.6 σ discrepancy between measured value of the muon anomalous magnetic moment and its prediction in the Standard Model [40]. In order to understand dark matter from properties of holographic systems, new holographic metal/superconductor transition models were constructed in the background of this dark matter gravity, for references see [41, 42]. The interesting topics of effects of dark matter on holographic vortices and holographic fluid viscosity were also carried out in [43, 44]. Since the holographic superconductor provides a lot of qualitative characteristic properties shared by real superconductor, it is believed that holographic superconductor theory may be applied to superconductor in the laboratory. As a further step along this line, some possible methods to directly detect the dark matter in the lab were proposed according to holographic theory [45]. Another interest to study this model is related to the question of possible matter configurations in AdS spacetime [46, 47]. On the sides of CFT on the boundary, it was shown that the dark matter sector really provides richer physics in the critical temperature and also the stability of metal/superconductor transitions on the boundary. Most surprisingly, for a certain set of parameters, there is a novel phenomenon of retrograde condensation in holographic dark matter sector found in Refs. [41, 42], which was already observed in other metal/superconductor systems [48, 49]. We further obtained the general conditions for retrograde condensations and proved retrograde condensations to be unstable in the s-wave metal/superconductor transitions [50]. In this work, we mainly focus on the effects of the dark matter in holographic insulator/superconductor model, which is interesting because the method provides the insight into the strong coupling system and possibly it enables findings of some 'experimental' facts connected with dark sector.

Most of holographic models were constructed in the background of AdS black hole or described metal/superconductor transitions. So the holographic insulator/superconductor transition in the AdS soliton spacetime needs much more research. Along this line, the dark matter sector was also considered in the AdS soliton spacetime while neglecting the matter fields' backreaction on the metric [51–53]. It was shown that the critical chemical potential is independent of the dark matter sector parameter without backreaction. In this work, we will show that the dark matter sector could affect the critical chemical potential and also the order of transitions when including backreaction. In contrast to retrograde condensation in holographic metal/superconductor models [41, 42, 48, 49], we will also manage to obtain the novel retrograde condensation in our s-wave holographic insulator/superconductor model.

On the other hand, the entanglement entropy is usually applied to keep track of the degrees of freedom for strongly coupled system while other traditional methods might not be available. According to the AdS/CFT correspondence, it was proposed that the holographic entanglement entropy of a strongly interacting system on the boundary can be calculated from a weakly coupled gravity dual in the bulk [54, 55]. With this elegant approach, the holographic entanglement entropy has recently been used to study properties of phase transitions in various holographic models and it provides us richer insights into the phase transitions [56]-[74]. For example, it was argued that the entanglement entropy is a good probe to the critical phase transition point and also the order of phase transitions. As a further step, we would like to examine whether the holographic entanglement entropy is still useful in disclosing properties of transitions in this general holographic insulator/superconductor model with dark matter sector.

This paper is organized as follows. In the next section, we introduce the holographic model with dark matter sector in the background of AdS soliton away from the probe limit. In part A of section III, we study the stability of holographic phase transitions. And in part B and part C of section III, we disclose properties of insulator/superconductor transitions by examining in detail behaviors of the scalar operator and the holographic entanglement entropy of the system. We will summarize our main results in the last section.

II. EQUATIONS OF MOTION AND BOUNDARY CONDITIONS

In this work, we consider holographic phase transitions with dark matter sector in the 5-dimensional AdS soliton spacetime. The general Lagrange density constructed by a scalar field and two U(1) gauge fields coupled in the gravitational background reads [41]

$$\mathcal{L} = R + \frac{12}{L^2} - \left(\frac{1}{4}F^{MN}F_{MN} + |\nabla_M\psi - iqA_M|^2 + m^2\psi^2 + \frac{1}{4}B^{MN}B_{MN} + \frac{\alpha}{4}B^{MN}F_{MN}\right),\tag{1}$$

where $\psi(r)$ is the complex scalar field, A_M stands for the ordinary Maxwell field and another additional U(1) gauge field B_M corresponds to the dark matter field, which is not completely decoupled with the visible matter. $-6/L^2$ is the negative cosmological constant, where L is the radius of AdS spactime which will be scaled unity in the following numerical calculation. m is the mass of the scalar field, q is the scalar charge and α is the coupling parameter between the two U(1) gauge fields.

The Einstein equations for the system can be written in the form

$$R_{MN} - \frac{1}{2}g_{MN}R - 6g_{MN} = \frac{1}{2}\tilde{T}_{MN},$$
(2)

where \tilde{T}_{MN} is the energy-momentum tensor expressed as

$$\tilde{T}_{MN} = F_{M\beta}F_N^{\beta} + B_{M\beta}B_N^{\beta} + \alpha B_{M\beta}F_N^{\beta} + 2\nabla_M\psi\nabla_N\psi + 2q^2A_MA_N\psi^2 + g_{MN}\left(-\frac{1}{4}F_{MN}F^{MN} - \frac{1}{4}B_{MN}B^{MN} - \frac{\alpha}{4}F_{MN}B^{MN} - \nabla_M\psi\nabla_M\psi - q^2A_MA^M\psi^2 - m^2\psi^2\right).$$
(3)

With the variation of the considered matter fields, we obtain the corresponding independent equations of motion in the form

$$\nabla_M F^{MN} - 2q^2 A^N \psi^2 + \frac{\alpha}{2} \nabla_M B^{MN} = 0, \qquad (4)$$

$$\nabla_M \nabla^M \psi - q^2 A_M A^M \psi - m^2 \psi = 0, \qquad (5)$$

$$\nabla_M B^{MN} + \frac{\alpha}{2} \nabla_M F^{MN} = 0. \tag{6}$$

Putting (6) into (4), we can eliminate the dark matter field and obtain the equation

$$\nabla_M F^{MN} - \frac{2q^2\psi^2 A^N}{\tilde{\alpha}} = 0, \tag{7}$$

where $\tilde{\alpha} = 1 - \frac{\alpha^2}{4}$.

Substituting (7) into (6), we arrive at

$$\nabla_M B^{MN} + \frac{\alpha q^2 \psi^2 A^N}{\tilde{\alpha}} = 0.$$
(8)

From Eqs. (7) and (8), we find that the ordinary Maxwell field A_M and the U(1) gauge field B_M which corresponds to the dark matter field share similar features for the holographic superconductor system in AdS soliton background, so we can still use the metric ansatz given in Ref. [8] where the authors took the backreaction into account (without dark matter sector), i.e.,

$$ds^{2} = -r^{2}e^{C(r)}dt^{2} + \frac{dr^{2}}{r^{2}B(r)} + r^{2}dx^{2} + r^{2}dy^{2} + r^{2}B(r)e^{D(r)}d\chi^{2},$$
(9)

$$A = \phi(r)dt, \qquad B = \eta(r)dt, \qquad \psi = \psi(r). \tag{10}$$

In order to get smooth solutions at the tip r_s satisfying $B(r_s) = 0$, we have to impose on the coordinate χ a period Γ as

$$\Gamma = \frac{4\pi e^{-D(r_s)/2}}{r_s^2 B'(r_s)}.$$
(11)

We also need $C(r \to \infty) = 0$ and $D(r \to \infty) = 0$ to recover the AdS boundary.

From above assumptions, we can obtain the equations of motion as

$$\psi'' + \left(\frac{5}{r} + \frac{B'}{B} + \frac{C'}{2} + \frac{D'}{2}\right)\psi' + \frac{q^2\phi^2 e^{-C}}{r^4 B}\psi - \frac{m^2}{r^2 B}\psi = 0,$$
(12)

$$\phi'' + \left(\frac{3}{r} + \frac{B'}{B} - \frac{C'}{2} + \frac{D'}{2}\right)\phi' - \frac{2q^2\psi^2}{\tilde{\alpha}r^2B}\phi = 0,$$
(13)

$$\eta'' + \left(\frac{3}{r} + \frac{B'}{B} - \frac{C'}{2} + \frac{D'}{2}\right)\eta' + \frac{\alpha q^2 \psi^2 \phi}{\tilde{\alpha} r^2 B} = 0, \tag{14}$$

$$C'' + \frac{1}{2}C'^2 + \left(\frac{5}{r} + \frac{A'}{2} + \frac{B'}{B}\right)C' - \frac{e^{-C}}{r^2}\left(\phi'^2 + \eta'^2 + \alpha\phi'\eta'\right) - \frac{2q^2\phi^2\psi^2e^{-C}}{r^4B} = 0,$$
(15)

$$B'\left(\frac{3}{r} - \frac{C'}{2}\right) + B\left[\psi'^2 - \frac{1}{2}A'C' + \frac{e^{-C}}{2r^2}\left(\phi'^2 + \eta'^2 + \alpha\phi'\eta'\right) + \frac{12}{r^2}\right] + \frac{q^2\phi^2\psi^2e^{-C}}{r^4} + \frac{m^2\psi^2}{r^2} - \frac{12}{r^2} = 0, \quad (16)$$

$$D' = \frac{2r^2C'' + r^2C'^2 + 4rC' - 2e^{-C}(\phi'^2 + \eta'^2 + \alpha\phi'\eta') + 4r^2\psi'^2}{r(6 + rC')},$$
(17)

where the prime denotes the derivative with respect to r. Since the equations are nonlinear and coupled to each other, we have to solve these equations by using the numerical shooting method which will integrate the equations of motion from the tip of the soliton out to the infinity. Thus, we have to specify the boundary conditions for this system. At the tip, we can impose proper boundary conditions as

$$\psi(r) = \psi_0 + \psi_1(r - r_s) + \cdots, \quad \phi(r) = \phi_0 + \phi_1(r - r_s) + \cdots,$$

$$\eta(r) = \eta_0 + \eta_1(r - r_s) + \cdots, \qquad B(r) = B_0(r - r_s) + \cdots,$$

$$C(r) = C_0 + C_1(r - r_s) + \cdots, \qquad D(r) = D_0 + D_1(r - r_s) + \cdots,$$
(18)

where the dots denote higher order terms.

After putting expansions (18) into (12) – (17) and considering leading terms of these equations, we are left with six independent parameters r_s , ψ_0 , ϕ_0 , η_0 , C_0 and D_0 at the tip. Near the AdS boundary $(r \to \infty)$, the asymptotic behaviors of the solutions are

$$\psi \to \frac{\psi_{-}}{r^{\lambda_{-}}} + \frac{\psi_{+}}{r^{\lambda_{+}}} + \cdots, \quad \phi \to \mu - \frac{\rho}{r^{2}} + \cdots, \quad \eta \to \xi - \frac{\varpi}{r^{2}} + \cdots,$$
$$B \to 1 + \frac{B_{4}}{r^{4}} + \cdots, \quad C \to \frac{C_{4}}{r^{4}} + \cdots, \quad D \to \frac{D_{4}}{r^{4}} + \cdots, \tag{19}$$

with $\lambda_{\pm} = (2 \pm \sqrt{4 + m^2})$. μ and ρ can be interpreted as the chemical potential and charge density in the dual theory respectively. The other two operators ξ and ϖ are dual to the U(1) gauge field $\eta(r)$.

From the equations of motion for the system, we obtain the scaling symmetry

$$r \to ar,$$
 $(\chi, x, y, t) \to (\chi, x, y, t)/a,$ $\phi \to a\phi,$ $\eta \to a\eta,$ (20)

which can be used to set $r_s = 1$ in the following calculation.

We will impose four constraint conditions at infinity. The asymptotic expressions (19) imply two constraint conditions at infinity: $C(\infty) = 0$ and $D(\infty) = 0$. We also have to impose one falloff of the scalar fields vanishes in order to get a stable CFT on the boundary. Choosing $m^2 = -\frac{15}{4} > -4$ above the BF bound [75], the second mode ψ_+ is always normalizable. In this paper, we will fix $\psi_- = 0$ and use the operator $\psi_+ = \langle O_+ \rangle$ to describe the phase transition in the dual CFT. For different values of ψ_0 , we can rely on the independent parameters ϕ_0 , η_0 , C_0 and D_0 as the shooting parameter to search for the solutions with the boundary conditions $\psi_- = 0$, $C(r \to \infty) = 0$, $D(r \to \infty) = 0$ and $\frac{\xi}{\mu}$ fixed.

III. HOLOGRAPHIC PHASE TRANSITIONS IN ADS SOLITON BACKGROUND

A. Stability of the scalar condensation

In this part, we investigate the stability of holographic insulator/superconductor phase transitions through the behaviors of the scalar operator. We choose the example $\Gamma = \pi$, $m^2 = -\frac{15}{4}$, q = 2, $\alpha = 2.5$ and $\frac{\xi}{\mu} = -1$ in Fig. 1. It is surprising in the left panel that the condensed phases appear at small chemical potential $\mu < \mu_c = 0.944$, which is different from the normal results in [7, 21]. We refer this phenomenon as the retrograde condensation, which was also observed in the holographic metal/superconductor transitions in the background of AdS black hole [41, 50]. By choosing different sets of parameters, we find that there are retrograde condensations for all superconducting solutions satisfying $\frac{\xi}{\mu} = -1$ and $\alpha > 2$.

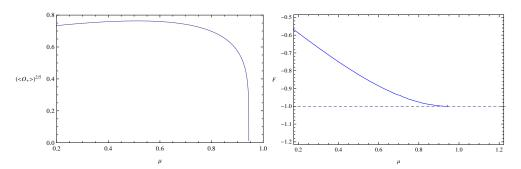


FIG. 1: (Color online) The phase transition in cases of $\Gamma = \pi$, $m^2 = -\frac{15}{4}$, q = 2, $\alpha = 2.5$ and $\frac{\xi}{\mu} = -1$. The left panel shows the behavior of the scalar condensation. The right panel represents the free energy of the system, where the solid line corresponds to the superconducting phase and the dashed line is with the normal phase.

In order to determine whether the retrograde condensation is thermodynamically favored, we should calculate the free energy of the system for both normal phase and condensed phase. We show the corresponding free energy of the system in the right panel of Fig. 1. It shows that the free energy of this hairy AdS soliton is larger than the free energy of the soliton in normal phase. Since the physical procedure corresponds to the phases with the lowest free energy, we arrive at a conclusion that the retrograde condensation superconducting solutions are thermodynamically unstable and the unusual behaviors of the scalar operator can be used to detect the thermodynamical instability of phase transitions. In the retrograde condensation, the soliton superconductor phase is not thermodynamically favored. In other words, there is no soliton/soliton superconductor transition as usual. In this case, we expect that there maybe interesting soliton/black hole and soliton/black hole superconductor transitions with the increase of chemical potential. And we plan to draw the complete diagram of the soliton/black hole/black hole superconductor system in the next work. And on the aspects of bulk theory, the unstable condensation also means the scalar field can't condense in the background of AdS soliton, which corresponds to an approach from the CFT on the boundary to the AdS gravity in the bulk.

Now we study the case of $\Gamma = \pi$, $m^2 = -\frac{15}{4}$, q = 2, $\alpha = 0.5$ and $\frac{\xi}{\mu} = 1$ in Fig. 2. In the left panel, we find a critical chemical potential $\mu_c = 0.944$ above which there is scalar condensation. In order to further study the phase transition, we plot the free energy in the right panel of Fig. 2. The free energy of superconducting state lies below the free energy of the normal state, which suggests that the superconducting solutions are thermodynamically stable. More calculations show that phase transitions are thermodynamically stable for all $\alpha > 0$ and $\frac{\xi}{\mu} = 1$. When $\frac{\xi}{\mu} = -1$, there are thermodynamically stable solutions for $0 \leq \alpha < 2$.

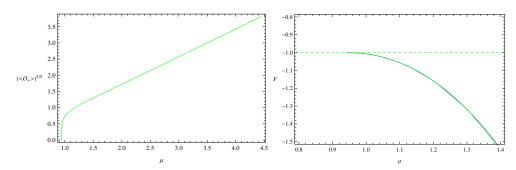


FIG. 2: (Color online) The phase transitions in cases of $\Gamma = \pi$, $m^2 = -\frac{15}{4}$, q = 2, $\alpha = 0.5$ and $\frac{\xi}{\mu} = 1$. The left panel represents the scalar operator with respect to the chemical potential. The solid green line in the right panel shows the free energy of the superconducting phase and the dashed line corresponds to normal phases. As a comparison, we also plot the results of equation (21) with solid blue line in the right panel.

With fitting methods, we obtain approximate formulas for the free energy of normal state (F_{SL}) and superconducting state (F_{SC}) that:

$$F_{SL} \approx -1.00, \quad F_{SC} \approx -1.00 - 2.21(\mu - \mu_c)^2 - 0.86(\mu - \mu_c)^3.$$
 (21)

In the right panel, the solid blue line corresponding to formula (21) almost coincides with the solid green line obtained from the original data. That means our fitting formula is valid. More importantly, the front formulas suggest that: $F_{SL}|_{\mu=\mu_c} = F_{SC}|_{\mu=\mu_c}, \frac{\partial F_{SL}}{\partial \mu}|_{\mu=\mu_c} = \frac{\partial F_{SC}}{\partial \mu}|_{\mu=\mu_c}, \frac{\partial^2 F_{SL}}{\partial \mu^2}|_{\mu=\mu_c} \neq \frac{\partial^2 F_{SC}}{\partial \mu^2}|_{\mu=\mu_c}$. In other words, the curve representing the physical phases with the lowest free energy is smooth at the critical point μ_c or the insulator/superconductor transition is of the second order.

B. Properties of the scalar condensation with weak backreaction

According to the transformation in [26], larger scalar charge q corresponds to cases of smaller backreaction parameter. In the following discussion, we take q = 2 as phases with weak backreaction in this part and q = 1 as the strong backreaction cases in the next part. We show the scalar operator $\langle O_+ \rangle^{1/\lambda_+}$ as a function of μ with $\Gamma = \pi$, $m^2 = -\frac{15}{4}$ and q = 2 in Fig. 3. It is shown that there are phase transitions at critical chemical potentials, above which the charged scalar condensation turns on. We exhibit the condensation of the scalar operator by choosing various α from top to bottom as: $\alpha = 0$, $\alpha = 0.5$, $\alpha = 1.0$ and $\frac{\xi}{\mu} = 1$. The increase of the parameter α develops shallower condensation gap. And in both curves, the critical chemical potential keeps as a constant $\mu_c = 0.944$ for different values of α . In all, the effects of the dark matter sector on the critical phase transition points and condensation gap are very different from those reported in the metal/superconductor system [41, 42, 50]. We conclude that the effects of the dark matter sector on transitions depend on backgrounds.

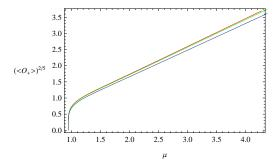


FIG. 3: (Color online) The phase transition in the cases of $\Gamma = \pi$, $m^2 = -\frac{15}{4}$ and q = 2. It shows the behavior of scalar operator with $\frac{\xi}{\mu} = 1$ and various α from top to bottom as: $\alpha = 0$ (red), $\alpha = 0.5$ (green) and $\alpha = 1$ (blue).

In the following, we pay attention to the holographic entanglement entropy(HEE) of the transition system. The authors in Refs. [54, 55] have provided a method to compute the entanglement entropy of conformal field theories (CFTs) from the gravity side. For simplicity, we consider the entanglement entropy for a half space corresponding to a subsystem \bar{A} defined by x > 0, $-\frac{R}{2} < y < \frac{R}{2}$ $(R \to \infty)$, $0 \le \chi \le \Gamma$. Then the entanglement entropy can be expressed as [67–69]:

$$S_{\bar{A}}^{half} = \frac{R\Gamma}{4G_N} \int_{r_0}^{\frac{1}{\varepsilon}} r e^{\frac{D(r)}{2}} dr = \frac{R\pi}{8G_N} (\frac{1}{\varepsilon^2} + S),$$
(22)

where $r = \frac{1}{\varepsilon}$ is the UV cutoff. The first term is divergent as $\varepsilon \to 0$. In contrast, the second term does not depend on the cutoff and thus is physical important. As a matter of fact, this finite term is the difference between the entanglement entropy in the pure AdS soliton and the pure AdS space. S = -1 corresponds to the pure AdS soliton.

We present the holographic entanglement entropy as a function of the chemical potential μ in Fig. 4 with $\Gamma = \pi$, $m^2 = -\frac{15}{4}$, q = 2, $\frac{\xi}{\mu} = 1$ and with various α . For all set of parameters, we find a threshold chemical potential $\mu = 0.944$, above which the hairy soliton appears. The jump of the slop of the entanglement entropy at $\mu = 0.944$ signals that some kind of new degrees of freedom like the Cooper pair would emerge in the new phase. It also can be easily seen from the pictures that when the parameters are fixed, the entanglement entropy first increases and then decreases monotonously as we choose a larger chemical potential. It means that there is firstly a increase and then a reduction in the number of degrees of freedom due to the condensate generated in the phase transitions [73]. We also see that larger α corresponds to smaller maximum entanglement entropy. Most importantly, we mention that compared with the scalar operator, the entanglement entropy is more

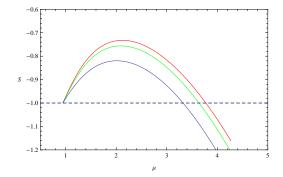


FIG. 4: (Color online) The holographic entanglement entropy as a function of the chemical potential μ for $\Gamma = \pi$, $m^2 = -\frac{15}{4}$ and q = 2. The dashed lines correspond to the entanglement entropy of a pure AdS soliton and the solid lines correspond to cases of superconducting solutions. We have choose $\frac{\xi}{\mu} = 1$ and various α from top to bottom as: $\alpha = 0$ (red), $\alpha = 0.5$ (green) and $\alpha = 1.0$ (blue).

sensitive to the change of the coupling parameter α .

The critical phase transition point $\mu = 0.944$ obtained from the behaviors of holographic entanglement entropy is equal to the threshold chemical potential $\mu_c = 0.944$ obtained from the behaviors of the free energy and the scalar operator. That means the holographic entanglement entropy can be used to search for the critical chemical potential. With detailed analysis of the holographic entanglement entropy, we conclude that the critical chemical potential is independent of the dark matter sector parameter. This numerical result is nontrivial since when considering the matter fields' backreaction on the metric, the equations of motion depend on the coupling parameter α even at the phase transition points where the scalar field is zero. And the jump of the slope of holographic entanglement entropy corresponds to second order phase transitions in the general holographic superconductor model with dark matter sector. In summary, we conclude that the entanglement entropy can be used to determine the critical phase transition point, the order of the phase transition and the values of the coupling parameter α . So the entanglement entropy is indeed a good probe of insulator/superconductor phase transitions with dark matter sector.

C. Various phase transitions with strong backreaction

Now we pay attention to the holographic superconductor with small charge q = 1 or strong backreaction. We exhibit the free energy as a function of the chemical potential in Fig. 5 with $\Gamma = \pi$, $m^2 = -\frac{15}{4}$ and various α . It can be seen from the left panel that, for the small model parameter $\alpha = 0.1$, F develops a discontinuity in the first derivative of the free energy with respect to the chemical potential at a critical value $\mu_c = 1.82$, which implies the first order phase transition. In the middle panel with $\alpha = 1.0$, F decreases smoothly near the critical point $\mu_c = 1.89$ indicating the second order phase transitions from normal state into superconducting state. What's more, besides the second order phase transition at $\mu_c = 1.89$, the free energy develops a "swallow tail" at $\mu = 2.08$ within the superconducting phase, a typical signal for a first order phase transition. The right panel shows that when the coupling parameter is larger as $\alpha = 1.5$, there is only second order insulator/superconductor phase transitions at the critical phase transition point $\mu_c = 1.89$. We conclude that the dark matter sector can affect the critical phase transition points and also the order of phase transitions.

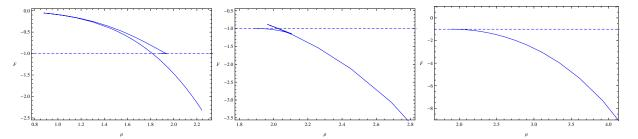


FIG. 5: (Color online) The free energy with respect to the chemical potential in cases of $\Gamma = \pi$, $m^2 = -\frac{15}{4}$, q = 1 and $\frac{\xi}{\mu} = 1$. The panels from left to right represent the cases of $\alpha = 0.1$, $\alpha = 1.0$ and $\alpha = 1.5$. The solid line corresponds to the superconducting phase and the dashed line of S = -1 is with the normal phase.

We also detect properties of phase transitions by studying the corresponding behaviors of the scalar operator in Fig. 6. In the left panel with $\alpha = 0.1$, at the critical chemical potential $\mu_c = 1.82$, the scalar operator $\langle O_+ \rangle^{1/\lambda_+}$ has a jump from insulator state to superconductor state indicating a first order phase transition. When choosing $\alpha = 1.0$ in the middle panel, the curves firstly increase continuously around the insulator/superconductor points $\mu_c = 1.89$ and then have a jump at $\mu = 2.08$ in the superconducting state. It means there are second order phase transitions at $\mu_c = 1.89$ and then first order phase transitions at $\mu = 2.08$. In cases of lager parameter $\alpha = 1.5$ in the right panel, $\langle O_+ \rangle^{1/\lambda_+}$ increases continuously with chemical potential, which is a classical performance of the second order phase transition.

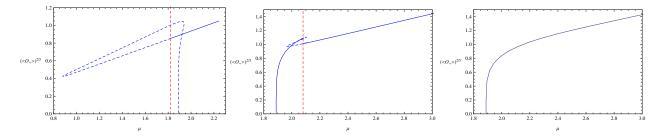


FIG. 6: (Color online) The behaviors of scalar operator in cases of $\Gamma = \pi$, $m^2 = -\frac{15}{4}$, q = 1 and $\frac{\xi}{\mu} = 1$. The panels from left to right show the case of $\alpha = 0.1$, $\alpha = 1.0$ and $\alpha = 1.5$. The blue solid lines correspond to the physical superconducting states

At last, we turn to study the holographic phase transition through the entanglement entropy approach. We plot the corresponding entanglement entropy with respect to the chemical potential μ in Fig. 7 with $\alpha = 1.0$

as an example. The blue dashed line S = -1 describes the entanglement entropy of the normal phase, while the blue solid line corresponds to the entanglement entropy of the superconducting phase. The holographic entanglement entropy is continuously at the critical chemical potential $\mu = 1.89$ and there are discontinuous slops at this transition point, which implies the phase transitions at $\mu = 1.89$ are of the second order. When we go on to increase the chemical potential, the entanglement entropy has a jump around $\mu = 2.08$ which corresponds to the "swallow tail" of the free energy F in Fig. 5 and the dump of the scalar operator in Fig. 6. The front phenomenon implies a first order phase transition around $\mu = 2.08$ in the superconducting phase. We state that the entanglement entropy can be used to study the critical phase transition points and the order of phase transitions in our general holographic superconductor model. It is clear that there is numerical noise in the picture. Since the numerical noise is small compared to the jump of the holographic entanglement entropy at the red dashed line, it will not change our results.

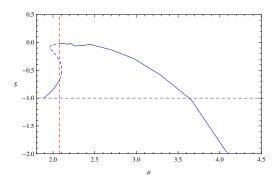


FIG. 7: (Color online) The entanglement entropy in cases of $\Gamma = \pi$, $m^2 = -\frac{15}{4}$, q = 1, $\alpha = 1.0$ and $\frac{\xi}{\mu} = 1$. The blue solid line shows the entanglement entropy of the superconducting phase and the blue dashed line S = -1 corresponds to normal phases.

IV. CONCLUSIONS

We studied holographic insulator/superconductor transition model with backreaction in the presence of dark matter sector. We disclosed properties of transitions through analyzing behaviors of the scalar operator and the holographic entanglement entropy of the system. For the case of weak backreaction, it was shown that the phase transition is of the second order and the larger coupling parameter α makes the gap of condensation lower. And the critical phase transition chemical potential is always a constant for different values of α similar to cases without backreaction. When including strong backreaction, the parameter α could affect the critical chemical potential and the order of phase transitions, which is very different from cases in the probe limit. In this case, we also found the jump of the holographic topological entanglement entropy corresponds to a first order transition in this general model with dark matter sector. More importantly, we observed novel phases refered as retrograde condensation due to the dark matter sector. In the retrograde condensation, the soliton superconductor phase is not thermodynamically favored. The front holographic properties of dark matter sector have potential application in dark matter detection and we plan to draw the complete diagram of the soliton/black hole/black hole superconductor/soliton superconductor system in the next work.

Acknowledgments

This work was supported by the National Natural Science Foundation of China under Grant Nos. 11305097, 11275066 and 11505066; the Shaanxi Province Science and Technology Department Foundation of China under Grant Nos. 2016JQ1039 and 2016JM1028; and the Hunan Provincial Natural Science Foundation of China under Grant No. 2016JJ1012. This work was also partly finished during the International Conference on holographic duality for condensed matter physics at Kavli Institute for Theoretical Physics China (KITPC), Chinese Academy of Sciences on July 6-31, 2015.

[12] F. Aprile and J.G. Russo, Models of Holographic superconductivity, Phys. Rev. D 81, 026009 (2010).

J.M. Maldacena, The large-N limit of superconformal field theories and supergravity, Adv. Theor. Math. Phys. 2, 231 (1998).

^[2] S.S. Gubser, I.R. Klebanov, and A.M. Polyakov, Gauge theory correlators from non-critical string theory, Phys. Lett. B 428, 105 (1998).

^[3] E. Witten, Anti-de Sitter space and holography, Adv. Theor. Math. Phys. 2, 253 (1998).

 ^[4] S.A. Hartnoll, Lectures on holographic methods for condensed matter physics, Class. Quant. Grav. 26, 224002 (2009).

^[5] C.P. Herzog, Lectures on Holographic Superfluidity and Superconductivity, J. Phys. A 42, 343001 (2009).

^[6] G.T. Horowitz, Introduction to Holographic Superconductors, Lect. Notes Phys. 828 313, (2011); arXiv:1002.1722 [hep-th].

^[7] T. Nishioka, S. Ryu, and T. Takayanagi, Holographic Superconductor/Insulator Transition at Zero Temperature, J. High Energy Phys. 1003, 131 (2010); arXiv:0911.0962 [hep-th].

^[8] G.T. Horowitz and B. Way, Complete Phase Diagrams for a Holographic Superconductor/Insulator System, J. High Energy Phys. 1011, 011 (2010); arXiv:1007.3714 [hep-th].

^[9] R. Gregory, S. Kanno, and J. Soda, Holographic Superconductors with Higher Curvature Corrections, J. High Energy Phys. 0910, 010 (2009).

^[10] L. Barclay, R. Gregory, S. Kanno, and P. Sutcliffe, Gauss-Bonnet Holographic Superconductors, J. High Energy Phys. 1012, 029 (2010).

^[11] Q. Pan, B. Wang, E. Papantonopoulos, J. Oliviera, and A. Pavan, Holographic Superconductors with various condensates in Einstein-Gauss-Bonnet gravity, Phys. Rev. D 81, 106007 (2010).

^[13] A. Salvio, Holographic superfluids and superconductors in dilaton gravity, J. High Energy Phys. **1209**, 134 (2012).

^[14] R. Cai and H. Zhang, Holographic Superconductors with Hořava-Lifshitz Black Holes, Phys. Rev. D 81, 066003 (2010).

^[15] J. Jing, Q. Pan, and S. Chen, Holographic Superconductors with Power-Maxwell field, J. High Energy Phys. 1111, 045 (2011).

^[16] G.T. Horowitz and M.M. Roberts, Holographic Superconductors with Various Condensates, Phys. Rev. D 78, 126008 (2008).

^[17] J. Sonner, A Rotating Holographic Superconductor, Phys. Rev. D 80, 084031 (2009).

 ^[18] Q. Pan and B. Wang, General holographic superconductor models with backreactions, arXiv:1101.0222 [hep-th].
 [19] S.A. Hartnoll, C.P. Herzog, and G.T. Horowitz, Holographic Superconductors, J. High Energy Phys. 0812, 015

⁽²⁰⁰⁸⁾

^[20] Y. Liu, Q. Pan, and B. Wang, Holographic superconductor developed in BTZ black hole background with backreactions, Phys. Lett. B 702, 94 (2011).

- [21] Y. Peng, Q. Pan, and B. Wang, Various types of phase transitions in the AdS soliton background, Phys. Lett. B 699, 383 (2011); arXiv:1104.2478 [hep-th].
- [22] J.P. Gauntlett, J. Sonner, and T. Wiseman, Holographic superconductivity in M-Theory, Phys. Rev. Lett. 103, 151601 (2009).
- [23] J. Jing and S. Chen, Holographic superconductors in the Born-Infeld electrodynamics, Phys. Lett. B 686, 68 (2010).
- [24] K. Maeda, M. Natsuume, and T. Okamura, Universality class of holographic superconductors, Phys. Rev. D 79, 126004 (2009).
- [25] X.H. Ge, B. Wang, S.F. Wu, and G.H. Yang, Analytical study on holographic superconductors in external magnetic field, J. High Energy Phys. 1008, 108 (2010).
- [26] Y. Brihaye and B. Hartmann, Holographic superconductors in 3+1 dimensions away from the probe limit, Phys. Rev. D 81, 126008 (2010).
- [27] C.P. Herzog, P.K. Kovtun, and D.T. Son, Holographic model of superfluidity, Phys. Rev. D 79, 066002 (2009).
- [28] D. Roychowdhury, AdS/CFT superconductors with Power Maxwell electrodynamics: reminiscent of the Meissner effect, Phys. Lett. B 718, 1089 (2013).
- [29] S. Franco, A.M. Garcia-Garcia, and D. Rodriguez-Gomez, A general class of holographic superconductors, J. High Energy Phys. 1004, 092 (2010).
- [30] S. Franco, A.M. Garcia-Garcia, and D. Rodriguez-Gomez, A holographic approach to phase transitions, Phys. Rev. D 81, 041901(R) (2010).
- [31] Q. Pan and B. Wang, General holographic superconductor models with Gauss-Bonnet corrections, Phys. Lett. B 693, 159 (2010).
- [32] Y. Peng, and Q. Pan, Stückelberg Holographic Superconductor Models with Backreactions, Commun. Theor. Phys. 59, 110 (2013).
- [33] D. Arean, L.A. Pando Zayas, I.S. Landea, and A. Scardicchio, The Holographic Disorder-Driven Supeconductor-Metal Transition, arXiv:1507.02280 [hep-th]
- [34] M. Baggioli and M. Goykhman, Phases of holographic superconductors with broken translational symmetry, J. High Energy Phys. 1507, 035 (2015).
- [35] H. Davoudiasl, H.-S. Lee, I. Lewis, and W.J. Marciano, "Dark" Z implications for parity violation, rare meson decays, and Higgs physics, Phys. Rev. D 85, 115019 (2012); C.-F. Chang, E. Ma, and T.-C. Yuan, Multilepton Higgs Deacays through the Dark Portal, J. High Energy Phys. 1403, 054 (2014).
- [36] A. Achucarro and T. Vachaspati, Semilocal and electroweak strings, Phys. Reports 327, 347 (2000); T. Vachaspati, Dark Strings, Phys. Rev. D 80, 063502 (2009); B. Hartmann and F. Arbabzadah, Cosmic strings interacting with dark strings, J. High Energy Phys. 07, 068 (2009); Y. Brihaye and B. Hartmann, Effect of dark strings on semilocal strings, Phys. Rev. D 80, 123502 (2009).
- [37] P. Jean et al., Early SPI/INTEGRAL measurements of 511 keV line emission from the 4th quadrant of the Galaxy, Astron. Astrophys. 407, L55 (2003).
- [38] J. Chang et al., An excess of cosmic ray electrons at energies of 300-800 GeV, Nature (London) 456, 362 (2008).
- [39] O. Adriani et al. (PAMELA Collaboration), An anomalous positron abundance in cosmic rays with energies 1.5-100 Gev, Nature 458, 607 (2009).
- [40] G.W. Bennett et al., Final report of the E821 muon anomalous magnetic moment measurement at BNL, Phys. Rev. D 73, 072003 (2006).
- [41] L. Nakonieczny and M. Rogatko, Analytic study on backreacting holographic superconductors with dark matter sector, Phys. Rev. D 90, 106004 (2014).
- [42] L. Nakonieczny, M. Rogatko, and K.I. Wysokinski, Magnetic field in holographic superconductor with dark matter sector, Phys. Rev. D 91, 046007 (2015).
- [43] M. Rogatko and K.I. Wysokinski, Holographic vortices in the presence of dark matter sector, J. High Energy Phys. 1512, 041 (2015).
- [44] M. Rogatko and K.I. Wysokinski, Viscosity of holographic fluid in the presence of dark matter sector, J. High Energy Phys. 1608, 124 (2016).
- [45] M. Rogatko and K.I. Wysokinski, Holographic superconductivity in the presence of dark matter: basic issues, Acta Phys. Polon. A 130, 558 (2016); arXiv:1603.02068 [physics].
- [46] T. Shiromizu, S. Ohashi, and R. Suzuki, No-go on strictly stationary spacetimes in four/higher dimensions, Phys. Rev. D 86, 064041 (2012).
- [47] B. Bakon and M. Rogatko, Complex scalar field in strictly stationary Einstein-Maxwell-axion-dilaton spacetime with negative cosmological constant, Phys. Rev. D 87, 084065 (2013).
- [48] F. Aprile, D. Roest, and J.G. Russo, Holographic Superconductors from Gauged Supergravity, J. High Energy Phys. 1106, 040 (2011).
- [49] R.-G. Cai, L. Li, and L.-F. Li, A Holographic P-wave Superconductor Model, J. High Energy Phys. 1401, 032 (2014).
- [50] Y. Peng, Holographic entanglement entropy in superconductor phase transition with dark matter sector, Phys. Lett. B 750, 420 (2015).
- [51] L. Nakonieczny, M. Rogatko, and K.I. Wysokinski, Analytic investigation of holographic phase transitions influenced by dark matter sector, Phys. Rev. D 92, 066008 (2015).
- [52] M. Rogatko and K.I. Wysokinski, P-wave holographic superconductor/insulator phase transitions affected by dark

matter sector, J. High Energy Physics 1603, 215 (2016).

- [53] M. Rogatko and K.I. Wysokinski, Condensate flow in holographic models in the presence of dark matter, J. High Energy Phys. 1610, 152 (2016).
- [54] S. Ryu and T. Takayanagi, Holographic Derivation of Entanglement Entropy from AdS/CFT, Phys. Rev. Lett. 96, 181602 (2006).
- [55] S. Ryu and T. Takayanagi, Aspects of Holographic Entanglement Entropy, J. High Energy Phys. 0608, 045 (2006).
- [56] T. Nishioka and T. Takayanagi, Entropy and Closed String Tachyons, J. High Energy Phys. 0701, 090 (2007).
- [57] I.R. Klebanov, D. Kutasov, and A. Murugan, Entanglement as a Probe of Confinement, Nucl. Phys. B 796, 274 (2008).
- [58] A. Pakman and A. Parnachev, Topological Entanglement Entropy and Holography, J. High Energy Phys. 0807, 097 (2008).
- [59] T. Nishioka, S. Ryu, and T. Takayanagi, Holographic Entanglement Entropy: An Overview, J. Phys. A 42, 504008 (2009).
- [60] L.-Y. Hung, R.C. Myers, and M. Smolkin, On Holographic Entanglement Entropy and Higher Curvature Gravity, J. High Energy Phys. 1104, 025 (2011).
- [61] J. de Boer, M. Kulaxizi, and A. Parnachev, Holographic Entanglement Entropy in Lovelock Gravities, J. High Energy Phys. 1107, 109 (2011).
- [62] N. Ogawa and T. Takayanagi, Higher Derivative Corrections to Holographic Entanglement Entropy for AdS Solitons, J. High Energy Phys. 1110, 147 (2011).
- [63] T. Albash and C.V. Johnson, Holographic Entanglement Entropy and Renormalization Group Flow, J. High Energy Phys. 1202, 095 (2012).
- [64] R.C. Myers and A. Singh, Comments on Holographic Entanglement Entropy and RG Flows, J. High Energy Phys. 1204, 122 (2012).
- [65] X.M. Kuang, E. Papantonopoulos, and B. Wang, Entanglement Entropy as a Probe to the Proximity Effect in Holographic Superconductors, J. High Energy Phys. 1405, 130 (2014).
- [66] Y. Peng and Q. Pan, Holographic entanglement entropy in general holographic superconductor models, J. High Energy Phys. 1406, 011 (2014).
- [67] R.-G. Cai, S. He, L. Li, and Y.-L. Zhang, Holographic Entanglement Entropy in Insulator/Superconductor Transition, J. High Energy Phys. 1207, 088 (2012); arXiv:1203.6620 [hep-th].
- [68] R.-G. Cai, S. He, L. Li, and L.-F. Li, Entanglement Entropy and Wilson Loop in Stückelberg Holographic Insulator/Superconductor Model, J. High Energy Phys. **1210**, 107 (2012); arXiv:1209.1019 [hep-th].
- [69] W.P. Yao and J.L. Jing, Holographic entanglement entropy in metal/superconductor phase transition with Born-Infeld electrodynamics, Nucl. Phys. B 889, 109 (2014).
- [70] Y. Peng and Y. Liu, A general holographic metal/superconductor phase transition model, J. High Energy Phys. 1502, 082 (2015).
- [71] T. Albash and C.V. Johnson, Holographic Studies of Entanglement Entropy in Superconductors, J. High Energy Phys. 1205, 079 (2012); arXiv:1202.2605 [hep-th].
- [72] B. Swingle and T. Senthil, Universal crossovers between entanglement entropy and thermal entropy, Phys. Rev. B 87, 045123 (2013).
- [73] R.-G. Cai, S. He, L. Li, and Y.-L. Zhang, Holographic Entanglement Entropy on P-wave Superconductor Phase Tansition, J. High Energy Phys. 1207, 027 (2012).
- [74] L.-F. Li, R.-G. Cai, L. Li, and C. Shen, Entanglement Entropy in a holographic P-wave Superconductor model, Nucl. Phys. B 894, 15 (2015).
- [75] P. Breitenlohner and D.Z. Freedman, Positive energy in Anti-de Sitter backgrounds and gauged extended supergravity, Phys. Lett. B 115, 197 (1982).